J. Iran. Chem. Soc., Vol. 8, No. 4, December 2011, pp. 908-918.

JOURNAL OF THE
Iranian
Chemical Society

Effects of Sugar Ring Puckering, Anti-Syn Interconversion and Intramolecular Interactions on N-Glycosidic Bond Cleavage in 3-Methyl-2´-deoxyadenosine and 2´-Deoxyadenosine

A. Ebrahimi*, M. Habibi-Khorassani and S. Bazzi
Department of Chemistry, University of Sistan and Baluchestan, P.O. Box 98135-674, Zahedan, Iran

(Received 9 December 2010, Accepted 11 February 2011)

The effects of structural parameters and intramolecular interactions on N-glycosidic bond length in 3-methyl-2´-deoxyadenosine (3MDA) and 2´-deoxyadenosine (DA) were investigated employing quantum mechanical methods. All calculations were performed at B3LYP/6-311++G** level in the gas phase. The N-glycosidic bond length strongly depends on sugar configuration; it is shorter in syn conformation relative to anti in many cases where they have the same sugar ring configuration. The sugar conformation can influence the N-glycosidic bond through interaction with the O4´ atom. The impact of intramolecular improper hydrogen bonds and H-H bonding interactions on N-glycosidic bond length was investigated in DA and 3MDA and their modeled structures. Improper hydrogen bonds decrease N-glycosidic bond length while H-H bonding interactions increase it.

Keywords: 3-Methyl-2´-deoxyadenosine, N-Glycosidic bond, Sugar ring puckering, Anti-syn interconversion, DNA repair enzyme, Improper hydrogen bond

INTRODUCTION

Deoxyribonucleic acid (DNA) damage is very frequent and appears to be a fundamental problem for life [1]. The cleavage of the N-glycosidic bond in deoxynucleosides and nucleosides is a common reaction in DNA damage and repair [2], toxicity mechanisms [3], and nucleobase salvage [4-6]. Depurination is a process in which the purine base (adenine or guanine) is removed from the deoxyribose sugar by hydrolysis of N-glycosidic bond. Most damaged bases can be removed and replaced in a process that begins with a glycosylase. For example, alkyl adenine DNA glycosidase (AAG) is responsible for recognizing and initiating the repair of a broad range of alkylated purines (damaged bases) including 3-methyl-2´-deoxyadenosine (3MDA) in human cells. Methylated nucleotides and N-glycosidic bond cleavage have been studied by different authors from both the experimental [7-22] and theoretical [23-26] points of view.

The inherent flexibility of sugar introduces major structural changes and causes important bearing on the biological function in the naturally occurring nucleic acids [27-29]. The two standard forms of right-handed DNA are principally defined by the sugar geometry; particularly north (C(3´)-endo) is a characteristic of A-DNA whereas south (C(2´)-endo) is a characteristic of B-DNA [30]. The conformational properties of deoxyadenosine (DA) and 3MDA have been studied by different researchers [31-34].

In the present study, the impacts of conformational changes, including sugar ring puckering and anti-syn interconversion that lead to different intramolecular

*Corresponding author. E-mail: Ebrahimi@hamoon.usb.ac.ir

interactions, on the N-glycosidic bond of 3MDA and DA have been investigated by quantum mechanical methods. The correlation between electronic properties and the N-glycosidic bond strength has been examined by means of natural bond orbital (NBO) and atoms in molecules (AIM) [36] analyses. A comparison of the most stable conformation of 3MDA with that of DA may be useful for evaluating the role of conformational changes in alkylated base recognition by DNA repair enzymes.

METHODS AND MODEL

DA and 3MDA can be modeled by replacing the sugar phosphate backbone and 3´-hydroxyl group with the hydrogen atoms (Scheme 1). One of the parameters defining the mononucleotide conformation is the dihedral angle about the N-glycosidic bond between the sugar and base ($\varphi_{O4'C1'N9C8}$ in Scheme 1). The two possible orientations of the base with respect to the sugar are termed syn ($\varphi_{O4'C1'N9C8} \approx 180$) and anti ($\varphi_{O4'C1'N9C8} \approx 60$) that are denoted **1** and **2** in DA, **1´** and **2´** in model DA, **m1** and **m2** in 3MDA, and **m1´** and **m2´** in model 3MDA conformations, respectively. Adenosine can exist either in syn (closed) or anti (open) form, and the interconversion between these two conformations is achieved by the pivot move around the N-glycosidic bond [37,38].

The sugar ring in adenosine may exist in the north type (C(2´)-exo and C(3´)-endo) or south type (C(2´)-endo and C(3´)-exo) [39,40]. **a** and **b** are used for north and south conformations, respectively, and **c** is used for those that cannot be specified by **a** or **b** index (see Scheme 1). Likewise, the pseudo-rotation angle P is used to define the conformational distribution of the sugar ring [40,41]. **a** conformers comprise all conformations that occupy the north half of the pseudo-rotational circle (P = 0 ± 90°) and **b** conformers occupy the southern half of the circle (p = 180 ± 90°) [40].

All geometries were optimized by the hybrid Hartree Fock density functional theory RB3LYP in conjunction with the 6-311++G** basis set using Gaussian03 program package. Frequency analysis was also performed at the same theoretical level. The absence of imaginary frequencies verified that all structures were true minima. The higher-level B3LYP/AUG-cc-pVDZ, MPWPW91/AUG-cc-pVDZ, MPWPW91/6-311++G**, MP2/AUG-cc-pVDZ, and MP2/6-311++G**

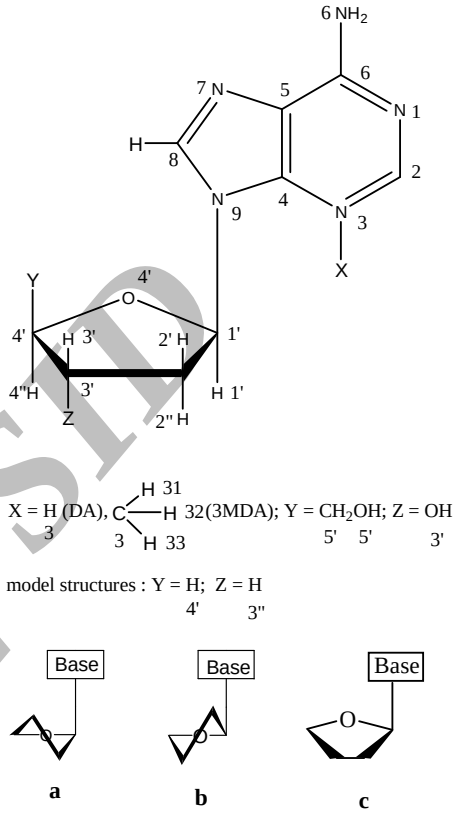

Scheme 1. Atomic numbering of DA, 3MDA, and model structures and the twist conformers of sugar ring.

Single point calculations were performed on geometries optimized at the above-mentioned level to investigate the dependence of the energy values on the level of calculation.

The solvent effect was treated by way of a polarizable continuum model (PCM) calculation using the integral equation formalism model (IEFPCM) [44] as implemented in Gaussian03 program package with a dielectric constant of 78.39 for H_2O.

The NBO and AIM analyses were performed on the wave functions obtained at 6-311++G** level of theory by NBO3.1 [45] and AIM2000 [46] programs.

RESULTS AND DISCUSSION

The results are presented in two subsections: one subsection corresponds to the 3MDA and DA (conformations are denoted as **m1a**, **m1b**, **m1c**, **m2a**, and **m2b** for 3MDA and

1a, **1b**, **2a**, and **2b** for DA) and the other corresponds to the model structures of 3MDA and DA (denoted as **m1´a**, **m1´b**, **m1´c**, **m2´a**, and **m2´b** for the model 3MDA and **1´a**, **1´b**, **2´a**, and **2´b** for the model DA). Where elongation or contraction of bonds due to the intramolecular interaction is reported, the lengths of bonds are compared with those in the structures that are free from that intramolecular interaction.

Model 3MDA

The relative energy E_{rel} decreased as the basis set changed from 6-311++G** to AUG-cc-pVDZ. The maximum change was equal to 0.61 kcal mol^{-1} (~19%) for **m2´b**. The change in relative energy was ~5% on changing the method from B3LYP to MPWPW91 that increases to ~40% on changing from B3LYP to MP2. In any case, the trend in the relative energies was almost independent of the method and basis set (see Table 1). In discussing the relationship between the relative energies and geometrical parameters, we use the results obtained at the B3LYP/6-311++G** level of theory. The order of the relative energies in the gas phase was **m1´c** > **m1´b** > **m2´b** > **m2´a** > **m1´a** at all levels of theory and was nearly identical to the trend in the solution media (the energy values of **m1´c** and **m1´b** are nearly identical in the solution). As can be seen in Table 1, the range of the relative energies in the solution (0-2.16 kcal mol^{-1}) is shorter than the range of the relative energies in the gas phase (0-3.65 kcal mol^{-1}). The dipole moments calculated at the above-mentioned level are also given in Table 1. The overall molecular polarity is expressed as the dipole moment and species with a higher dipole moment become more stable in polar solvents. Thus,

Table 1. The Relative Energies in kcal mol^{-1} and the Dipole Moments (D) in Debye

	B3LYP		MPWPW91		MP2		D
Model 3MDA							
m1´a	*0.00* (*0.00*)	*0.00*	0.00	*0.00*	0.00	*0.00*	2.17
m2´a	2.44 (0.71)	*2.00*	2.43	*1.93*	2.54	*2.17*	5.00
m1´b	3.64 (2.16)	*3.32*	3.76	*3.40*	3.90	*3.71*	2.65
m2´b	3.10 (1.58)	*2.60*	3.25	*2.64*	4.08	*3.71*	4.91
m1´c	3.65 (2.08)	*3.23*	3.76	*3.35*	3.86	*3.62*	2.54
Model DA							
1´a	0.53 (0.78)	*0.54*	1.01	*0.68*	1.14	*0.80*	3.72
2´a	0.05 (0.11)	*0.33*	0.15	*0.00*	0.00	*0.00*	4.39
1´b	0.00 (0.20)	*0.00*	0.00	*0.13*	0.35	*0.00*	3.66
2´b	0.83 (0.00)	*1.05*	1.19	*0.91*	1.83	*1.78*	5.37
3MDA							
m1a	1.10	*1.30*	1.21	*1.43*	0.00	*0.16*	
m2a	1.92	*1.81*	2.00	*1.82*	2.33	*2.13*	
m1b	2.35	*2.28*	2.60	*2.68*	2.16	*2.04*	
m2b	0.00	*0.00*	0.00	*0.00*	0.32	*0.00*	
m1c	2.35	*2.28*	2.60	*2.68*	2.16	*2.04*	
DA							
1a	2.69	*2.86*	2.88	*3.06*	3.26	*3.62*	
2a	5.83	*6.18*	6.02	*6.35*	6.18	*7.58*	
1b	0.00	*0.00*	0.00	*0.00*	0.00	*0.00*	
2b	5.77	*5.85*	6.08	*6.20*	6.16	*7.29*	

The italicized values calculated with the AUG-cc-pVDZ basis set and others calculated with 6-311++G** basis set. The data in the parentheses calculated in solution media.

the maximum difference between the relative energies in the solution media is lower than the gas phase and corresponds to the conformer that has the maximum dipole moment in each category. In the model 3MDA, the highest dipole moment and the largest difference between the relative energies in the gas phase and the solution media correspond to **m2´a**. Apart from $\varphi_{C4'C1'N9C8}$ dihedral angle (see Scheme 1), there is a meaningful relationship between the relative energy and sugar conformation; conformation **a**, is more stable than **b**, while **c** is in the highest energy level in the model 3MDA. Some geometrical parameters of different conformations are presented in Table 2. In both gas phase and solution media the order of N-glycosidic bond length (C1´-N9) is **m2a´** > **m1´a** > **m2´b** > **m1´b** > **m1´c**. Thus, except for $\varphi_{O4'C1'N9C8}$ dihedral angle, N-glycosidic bond length strongly depends on sugar conformation. As a result, the longest and shortest bonds correspond to **a** and **c** conformations, respectively.

The following is an account of how sugar conformation affects the glycosidic bond. The results of NBO analysis on the wave functions obtained at B3LYP/6-311++G** level are given in Table 3. The order of occupancy of $\sigma^*_{C1'N9}$ is **m2´a** > **m1´a** > **m2´b** > **m1´b** > **m1´c**, which is similar to the order of the bond length. The N-glycosidic bond length increases as the occupation number of $\sigma^*_{C1'N9}$ increases, therefore, the impact of $lp_{(O)} \rightarrow \sigma^*_{C1'N9}$ interaction that plays a significant role in the occupation number of $\sigma^*_{C1'N9}$ becomes more clear. The $lp_{(O)} \rightarrow \sigma^*_{C1'N9}$ interaction energy $E^{(2)}$ ranges from 1.70 to 13.22 kcal mol^{-1}. As can be seen in Table 3, the order of $E^{(2)}$ value is **m1´a** > **m2´a** > **m2´b** > **m1´b** > **m1´c**. The $E^{(2)}$ value depends on sugar conformation such that the trend in this value is similar to the trend in N-glycosidic bond length, *i.e.* **a** > **b** > **c**. Thus, the $O_{4'}$ atom strongly influences the N-glycosidic bond through $lp_{(O)} \rightarrow \sigma^*_{C1'N9}$ interaction upon conformational changes.

Table 2. Some Geometrical Parameters (in Å) for the Model and Nonmodel Structures

3MDA									
	m1´a	**m2´a**	**m2´b**	**m1´b**	**m1´c**	**m1a**	**m2a**	**m2b**	**m1c**
N9-C8	1.392	1.391	1.392	1.393	1.393	1.391	1.395	1.395	1.394
N9-C4	1.372	1.368	1.367	1.376	1.376	1.37	1.367	1.368	1.378
N9-C1´	1.500	1.509	1.498	1.476	1.471	1.498	1.502	1.478	1.469
(N9-C1´) $_{sol}$	1.499	1.507	1.495	1.475	1.469				
C1´-O4´	1.403	1.392	1.399	1.406	1.407	1.404	1.399	1.411	1.410
C1´-C2´	1.532	1.541	1.541	1.531	1.547	1.524	1.535	1.534	1.530
C8-H6	1.077	1.077	1.078	1.080	1.080	1.077	1.082	1.081	1.080
C2´-H2´	1.089	1.091	1.093	1.093	1.091	1.089	1.090	1.089	1.090
C3-H32	1.088	1.090	1.090	1.086	1.085	1.088	1.090	1.090	1.084
DA									
	1´a	**2´a**	**2´b**	**1´b**		**1a**	**2a**	**2b**	**1b**
N9-C8	1.384	1.382	1.382	1.383		1.383	1.384	1.385	1.384
N9-C4	1.386	1.380	1.378	1.385		1.383	1.379	1.382	1.382
N9-C1´	1.461	1.482	1.470	1.467		1.467	1.466	1.45	1.457
(N9-C1´) $_{sol}$	1.462	1.482	1.462	1.466					
C1´-O4´	1.420	1.408	1.416	1.415		1.412	1.422	1.431	1.418
C1´-C2´	1.545	1.532	1.542	1.548		1.542	1.536	1.535	1.534
C8-H6	1.081	1.078	1.078	1.081		1.081	1.080	1.080	1.081
C2´-H2´	1.089	1.088	1.093	1.089		1.090	1.089	1.090	1.090
N3-H5´						0.977	0.961	0.961	0.980

Table 3. The $lp_{(O)} \rightarrow \sigma^*_{C1'N9}$ Interaction Energy $E^{(2)}$ in kcal mol^{-1} and the Occupancy of $\sigma^*_{C1'N9}$ ($\times 10^2$) Calculated by the NBO Method at the B3LYP/6-311+ + G** Level

	$E^{(2)}$	n_σ*		$E^{(2)}$	n_σ*
1´b	11.43	6.49	**1b**	4.87	5.24
2´a	11.94	6.90	**2a**	8.76	6.09
1´a	7.48	5.96	**1a**	7.41	6.02
2´b	9.15	5.90	**2b**	1.49	4.99
m1´a	13.22	7.88	**m1a**	13.63	7.98
m2´a	12.70	7.91	**m2a**	11.14	7.48
m2´b	10.29	6.92	**m2b**	6.27	5.88
m1´b	3.87	5.46	**m1b**	0.97	4.91
m1´c	1.70	4.98	**m1c**	0.97	4.91

The ρ and $\nabla^2\rho$ values calculated by the AIM method at intramolecular bond critical points (BCPs) are given in Table 4. The C-H···H-C, C-H···O, N-C···H-C and C-C···H-C intramolecular interactions are observed in different conformations of model 3MDA (see Fig. 1 for two typical molecular graphs). The ρ and $\nabla^2\rho$ values calculated at BCPs of intramolecular interactions range from 5.406×10^{-3} to 16.978×10^{-3} au and 0.017 to 0.056 au, respectively.

In C-H···O interaction, $O_{4'}$ is proton acceptor and the nucleobase is proton donor. The contraction of the C-H bond (by 0.002 to 0.005 Å) and a concomitant blue shift (by 37.56 to 54.85 cm^{-1}; see Table 5) of the C-H stretching vibrational frequency can be the consequences of structural reorganization resulting from the elongation of bonds in the remote part of the proton donor (see Table 2). The value of changes is small, but due to the weakness of such intramolecular interactions, discussion about these changes is justifiable and confirmed experimentally in these systems [47]. The C-H stretching vibrational frequency in model 3MDA conformations is compared with that when the sugar is replaced with the H atom. So, the C-H···O interaction in the model 3MDA can be categorized as an improper hydrogen bond. Hobza [47] has investigated the nature of improper hydrogen bonds. According to the Hobza report, improper blue shifting hydrogen bonding of the type Z-X-H···Y is portrayed by a two-step process. First, electron density is transferred from the proton acceptor (Y) to the remote part of the proton donor (Z-X part of the Z-X-H···Y system). The electron density increase in the remote part of the proton donor leads to the elongation of bond(s) in the part of the system which in the second step is accompanied by a structural reorganization of the whole proton donor. The net effect of this reorganization is a contraction of the X-H bond with a concomitant increase (blue shift) in the X-H stretch frequency. The N-C···H-C and C-C···H-C interactions that are observed in anti conformations could be considered as electrostatic interactions between C and H atoms that possess disparate charges.

The N-glycosidic bond in anti conformations of the model 3MDA (1.498 and 1.509 Å in **m2´b** and **m2´a**) is longer than syn (**m1b** (1.476) and **m1a** (1.500) Å) when the sugar ring configuration is kept constant. Moreover, the O4´···H31-C3 improper hydrogen bond is only observed in syn configurations and the C4-N9 bond (in remote part of proton donor) in syn is longer than anti (by ~0.01 Å). Since the C4-N9 bond elongation is accompanied by the N-glycosidic bond contraction, the shorter glycosidic bond in syn relative to anti, can partly be attributed to the O4´···H31-C3 improper hydrogen bonds. On the other hand, the N-C···H-C and C-C···H-C electrostatic interactions do not have a significant effect on the N-glycosidic bond length in anti conformations.

An H···H intramolecular BCP is observed in the molecular graph obtained from the AIM analysis for each one of **m1´a**,

Table 4. The Values of $\rho_{BCP} \times 10^3$ and $\nabla^2\rho_{BCP}$ (in au) Calculated at the BCPs of Intramolecular Interactions

	ρ_{BCP}	$\nabla^2\rho_{BCP}$		ρ_{BCP}	$\nabla^2\rho_{BCP}$
m1´a			**m1´c**		
O4´-H31	15.176	0.055	O4´-H32	16.978	0.056
H2´-H6	11.047	0.046	H2´-H31	7.097	0.022
C1´-N9	234.506	-0.552	C1´-N9	249.119	-0.636
m2´a			**1´a**		
C2´H32	5.619	0.020	H2´-N3	7.564	0.028
H1"-C3	8.217	0.030	H3´-N3	10.035	0.030
C1´-N9	230.193	-0.531	C1´-N9	258.205	-0.683
m2´b			**1´b**		
H2"-H32	5.406	0.017	H2´-N3	9.943	0.033
H1"-C3	9.012	0.033	H4´-N3	7.102	0.020
C1´-N9	235.690	-0.563	C1´-N9	254.890	-0.660
m1´b			**2´a**		
O4´-H32	16.112	0.055	H2´-N3	7.953	0.026
H2´-H31	7.448	0.022	C1´-N9	248.306	-0.632
C1´-N9	246.098	-0.620	**2´b**		
			C1´-N9	254.748	-0.670

m2´b, **m1´b** and **m1´c** conformers. According to Tables 2 and 4, the N-glycosidic bond elongation is accompanied by the increases in $\rho_{H\cdots H}$ in the syn conformations.

Model DA

As seen in Table 1, the difference between the relative energies of conformations is lower than that in the model 3MDA. So, the trend in the energy values changes a little as the level changes. The most stable conformation is **1´b** that changes to **2´a** at the MPWPW91/AUG-cc-pVDZ and MP2/6-311++G** levels of theory. Herein, the most stable conformation is **1´b** at the B3LYP/6-311++G** level while it is **m1´a** in the model 3MDA. The relative energies of model DA conformations in the gas phase and solution media range from 0.00 to 0.83 and 0.00 to 0.78 (in kcal mol^{-1}), respectively. The range changes slightly from the gas phase to the solution media. The 3MDA conformations are at a lower energy level in the solution media relative to the gas phase.

The results of NBO analysis at B3LYP/6-311++G** level are displayed in Table 3. The $lp_{(O)} \rightarrow \sigma^*_{C1'N9}$ interaction energy $E^{(2)}$ ranges from 7.48 to 11.94 kcal mol^{-1} for different conformations of the model DA (see Table 3). The orders of $E^{(2)}$, occupation number of $\sigma^*_{C1'N9}$, and the N-glycosidic bond length in the gas phase are **2´a** (11.94) > **1'b** (11.43) > **2´b** (9.15) > **1´a** (7.48 kcal mol^{-1}), **2´a** (6.90) > **1´b** (6.49) > **1´a** (5.96) > **2´b** (5.90 e), and **2´a** (1.482) > **2´b** (1.470) > **1´b**

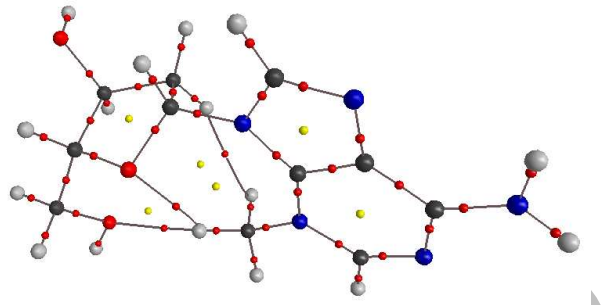

m1b

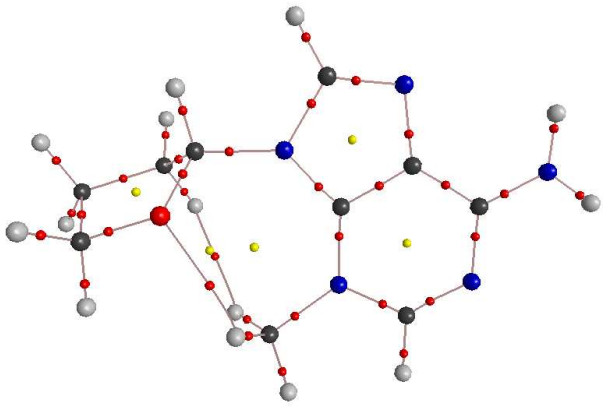

m1′b

Fig. 1. The molecular graphs of **m1´b** and **m1b** obtained from AIM analysis at the B3LYP/6-311++G** level of theory.

(1.467) > **1´a** (1.461 Å), respectively. In the solution media, the bond length in **1´b** (1.466 Å) is slightly greater than **2´b** (1.462 Å) (see Table 3). There are logical relationships between the N-glycosidic bond length, the occupation number of $\sigma^*_{C1'N9}$, the $E^{(2)}$ value of $lp_{(O)} \rightarrow \sigma^*_{C1'N9}$ interaction, and the sugar ring configuration in the model 3MDA conformations. However, there is not a meaningful relationship between these parameters in the model conformations of DA. The N-glycosidic bond length is not in logical relationship with the occupation number of $\sigma^*_{C1'N9}$, because the conformational changes that lead to different $lp_{(O)} \rightarrow \sigma^*_{C1'N9}$ interactions have an ambiguous impact on the N-glycosidic bond length. On the other hand, the effect of other parameters, such as rotation around the $\varphi_{O4'C1'N9C8}$ angle, that leads to different intramolecular interactions, on the N-glycosidic bond length is more than the effect of sugar ring puckering. The N-glycosidic bond in the anti conformation is longer than syn with the same sugar ring configuration.

The lengths of C-H bonds that interact with the N3 atom are shorter than 1.090 Å, but the lengths of other C-H bonds of sugar ring are longer than that value in all conformations of the model DA. The contraction of C-H bond and a concomitant blue shift of the C-H stretching vibrational frequency are consequences of the structural reorganization resulting from the elongation of bonds in the remote part of the proton donor. The C-H stretching vibrational frequency is compared with the corresponding value where the sugar ring is replaced with an H atom. The results are in agreement with the C-H···N intramolecular improper hydrogen bonds. What is the effect of these interactions on the N-glycosidic bond length.

Table 5. The Change of X-H Stretching Vibrational Frequency in cm^{-1}

Conformation	Δν	Conformation	Δν
m1´a(C3-H32)	37.56	m2a(C8-H6)	-60.77
m1´b(C3-H32)	54.85	m2b(C8-H6)	-44.31
m1´c(C3H32)	53.08	m2b(C2´-H2´)	11.27
1a(O5´-H5´)	-316.72	1´a(C2´-H2´, C3´-H3´)	38.61
1´b(C2´-H2´)	31.85	1b(N3- H2´,O5´-H2´)	10.74
1´b(C4´-H4´)	43.12	1b(O5´-H5´)	-384.89
2´a(C2´-H2´)	47.15	2a(C8-H6)	12.96
2´b(C2´-H2")	36.39	2a(C2'-H2´)	6.59
m1b(C3-H32)	18.17	2b(C8-H6)	13.64
m1c(C3-H32)	19.93	2b(C2´-H2´)	21.45

Δν = ν - ν(in the absence of XH···Y hydrogen bond).

There is a meaningful relationship between the N-glycosidic bond length and the sum of C1´-O4´ and C1´-C2´ bond lengths in all conformations. The improper hydrogen bonds can affect these bonds in the remote part of the proton donor. The above mentioned sum is higher and the length of N-glycosidic bond is shorter in the syn conformations relative to the anti because of an extra intramolecular improper hydrogen bond in the former. The longest C1´-O4´ and C1´-C2´ bonds and the shortest N-glycosidic bond correspond to **1´a** with H2´···N3 and H3´···N3 improper H-bonds, while the reverse is true for **2´a** without any improper H-bond. Similarly, the C2´-H2" bond is shorter than 1.090 Å and the C1´-O4´ and C1´-C2´ bonds in **2´b** are longer than **2´a**; thus, a shorter glycosidic bond can be predicted for **2´b**.

3MDA Conformations

Energetic details for the 3MDA conformations are presented in Table 1. Herein, **m2b** is the most stable conformer at all levels of theory with the exception of MP2/6-311++G**. The highest change in the ΔE value by changing the basis set from 6-311++G** to AUG-cc-pVDZ corresponds to **m2b** (by 0.32 kcal mol^{-1}).

Unlike the model 3MDA, no meaningful relationship is observed between the relative energies and sugar conformation in 3MDA because of new intramolecular interactions that are observed in the presence of OH and OCH_3 functional groups.

The results of NBO analysis on the wave functions obtained at B3LYP/6-311++G** level are given in Table 3. The trend in the $lp_{(O)} \rightarrow \sigma^*_{C1'N9}$ interaction energy is similar to the trend in the N-glycosidic bond length (**a** > **b** > **c**). This is similar to the result obtained for the conformations of the model 3MDA. The $lp_{(O)} \rightarrow \sigma^*_{C1'N9}$ interaction increases the occupation number of $\sigma^*_{C1'N9}$ that can affect the N-glycosidic bond length. Furthermore, the conformational changes likely influence the N-glycosidic bond through the intramolecular interactions between base moiety and the O4´ atom.

Though the N-glycosidic bond length increases on replacing the OH and OCH_3 groups by the H atom, identical trends are observed for that before and after modeling. A comparison of geometrical parameters of each conformation in 3MDA with those optimized after replacing the OH and OCH_3 with the H atom, which will be made below, will confirm the influence of intramolecular interactions on the N-glycosidic bond.

It can be observed from the AIM results that the H···H intramolecular interaction in **m1´a** is replaced by O5´···N9 electrostatic interaction in **m1a**; The O5´ and N9 atoms possess negative and positive charges, respectively. As mentioned earlier, H···H intramolecular interactions are accompanied by the N-glycosidic bond elongation, so in the absence of this interaction the N-glycosidic bond in **m1a** (by ≈0.002 Å) is shorter than **m1´a**.

In comparison with **m1´b**, an extra intramolecular

hydrogen bond is observed between O5′ and H32 in **m1b** that is accompanied by C3'-H32 contraction and N9-C4 elongation (Table 2). The C3′-H32 contraction comes along with a concomitant increase in C-H stretching vibrational frequency when compared with **m1'b** (18.17 cm^{-1}). The N-glycosidic bond in **m1b** is shorter than that in **m1′b** (by ≈0.007 Å) that could be attributed to the interaction in question.

Similarly, **m1c** possesses an extra intramolecular improper hydrogen bond between O5′ and H32 relative to **m1′c**. The C3-H32 contraction (by 0.001 Å), the blue shift of C3′-H32 stretching vibrational frequency (by 19.93 cm^{-1}), and the N9-C4 elongation (by 0.002 Å) (in remote part of proton donor) are observed in **m1c** relative to **m1′c**. The O5′ atom is proton acceptor and the nucleobase is proton donor. The N9-C4 elongation leads to the C1′-N9 contraction such that the latter bond in **m1c** becomes shorter than that in **m1'c** (by ≈0.002 Å).

The C2′···H32 electrostatic interaction in **m2′a** is replaced by the O5'···H6 interaction in **m2a**. The new interaction that leads to the C8-H6 elongation (by 0.005 Å) and a concomitant decrease in C8-H6 stretching vibrational frequency (by 60.77 cm^{-1}) relative to **m2′a** is categorized as a regular hydrogen bond. The O5'···H6 hydrogen bond is accompanied by an increase in the C8-N9 bond length (0.004 Å) that leads to the C1'-N9 bond contraction (0.007 Å) in **m2a** relative to **m2′a**. This explains why the N-glycosidic bond length in **m2a** is shorter than that in **m2′a** (by 0.007 Å).

The H···H interaction in **m2′b** is replaced by the O5′···H6 and O5′···H2′ interactions in **m2b**. The C8-H6 elongation in **m2b** (by 0.003 Å in comparison with **m2′a**) confirms that the O5′···H6 interaction is a regular hydrogen bond that is accompanied with the N9-C8 elongation (0.003 Å) and a concomitant decrease in the C8-H6 stretching vibrational frequency (by 44.31 cm^{-1}). The O5′···H2′ interaction could be considered as an improper hydrogen bond that causes contraction in the C2′-H2′ bond (by 0.004 Å), blue shift (11.27 cm^{-1}) in the stretching vibrational frequency, and expansion in the O4′-C1′ and C2′-C1′ bonds relative to **m2′b**. The N-glycosidic bond length in **m2b** is shorter than **m2′b** (by ≈0.020 Å) that can be accounted for by the absence of H···H interaction and the presence of O5′···H6 and O5′···H2′ interactions.

DA Conformations

As can be seen in Table 1, the energy values decrease as the basis set changes from 6-311++G** to AUG-cc-pVDZ. The maximum change is equal to 1.44 kcal mol^{-1} (~22.7%) for **2a**. The relative energy changes ~23% as the method changes from B3LYP to MP2 for **2b**, which is the greatest variation upon changing the method. The trend in the relative energies of conformers in DA is **1b** > **1a** > **2b** > **2a** that is different from that in the model DA. The most stable conformation in DA is **1b** while in 3MDA is **m2b**. The conformational difference in the most stable conformations of DA and 3MDA can be one of the most important parameters in alkylated base recognition by DNA repair enzymes.

The order of occupation number of $\sigma^*_{C1'N9}$ is **2a** > **1a** > **1b** > **2b** that is similar to the order of $E^{(2)}$ for $lp_{(O)} \rightarrow \sigma^*_{C1'N9}$ interaction. The increase in the occupation number of $\sigma^*_{C1'N9}$ leads to the increase in the N-glycosidic bond length. This observation confirms that the O4′···nucleobase interaction, which depends on sugar conformation, can affect the N-glycosidic bond length. Other intramolecular interactions can also affect the N-glycosidic bond length as already mentioned.

The comparison of each conformation in DA with that in the model DA confirms our previous results. The H2′···N3 improper hydrogen bond in **1′a** is replaced by the H5'···N3 hydrogen bond in **1a**. This hydrogen bond is accompanied by the elongation of O5′···H5′ bond and red shift in its stretching vibrational frequency (316.72 cm^{-1}). Thus, in the absence of H2'···N3 improper hydrogen bond, the O4′-C1′ and C2′-C1′ bonds become shorter and the N-glycosidic bond becomes longer (by ≈0.006 Å, in comparison with **1'a**).

The H2′···N3 and H4′···N3 improper hydrogen bonds are observed in the AIM results of **1′b**, while the H2′···N3 and O5′···H2′ improper hydrogen bonds and the H5'···N3 conventional hydrogen bonds are observed in **1b**. The changes in the stretching frequencies of proton donors are evidences for these interactions (see Table 5). The C2′-H2′ bond in **1b** is longer than **1′b**, whereas the O4′-C1′, C2′-C1′, and N-glycosidic bonds in **1b** are shorter than **1'b** (by ≈0.009 Å). The special triangular interaction in **1b** probably does not allow the N-glycosidic bond elongation (see Fig. 2).

The O5′···H6 interaction is observed in the AIM results of **2a** that is accompanied by the C8-N9 elongation (0.002 Å); this interaction is not observed in **2′a**. Although the H2′···N3 improper hydrogen bond cannot be seen in the AIM results of **2a**, the contraction of C2′-H2′ (0.001 Å) and the elongation of O4′-C1′ (0.014 Å) and C2′-C1′ (0.004 Å) are observed for

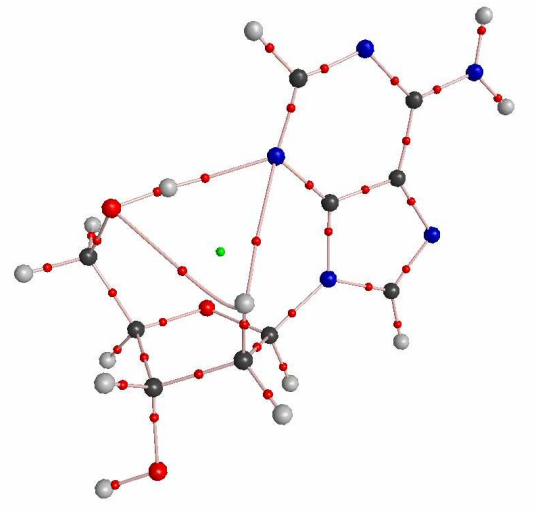

1b

Fig 2. The molecular graph of 1b obtained from AIM analysis at the B3LYP/6-311++G** level of theory.

that. In addition, an increase in the C2´-H2´ stretching vibrational frequency (6.59 cm^{-1}) is observed in comparison with **1a**. Thus, the O5´···H6 and H2´···N3 interactions decrease the N-glycosidic bond length because of the C8-N9, O4´-C1´ and C2´-C1´ elongation. The N-glycosidic bond length in **2a** is shorter than **2'a** (by ≈0.016 Å).

The O5´···H6 H-bond and the O5´···H2´ improper H-bond are observed in the AIM results of **2b**. The contraction of C2´-H2´ (0.003 Å), and the elongation of C8-N9 (0.003 Å) and O4´-C1´ (0.015 Å) are in agreement with those interactions. The blue shift is also observed in the stretching vibrational frequency of C2´-H2´ (21.45 cm^{-1}). Both interactions contract the N-glycosidic bond such that its length in **2b** becomes shorter than **2´b** (by ≈0.020 Å).

CONCLUSIONS

In the present study, the impacts of conformational changes, including sugar ring puckering and anti-syn interconversion, on the N-glycosidic bond of 3MDA and DA were investigated by the *ab initio* calculation and by NBO and AIM analyses. The order of the relative energies in the gas phase was nearly identical to the trend in the solution media. The most stable conformation in the model DA was different from that in the model 3MDA. This can be used to evaluate the role of conformational changes in the alkylated base recognition by DNA repair enzymes. The N-glycosidic bond length in the syn conformations was shorter than anti for 3MDA, the model 3MDA, and the model DA. The conformational changes can influence that bond through interaction with the O4´ atom. The C-H···N and C-H···O intramolecular interactions were observed for different conformations where all the C-H···N interactions could be categorized as the improper hydrogen bonds. The improper hydrogen bonds were accompanied with the enlargement of the other two bonds in the remote part of proton donor; the N-glycosidic bond contraction was observed when the remote part included one of the C1´-O4´, C1´-C2´, N9-C8 or N9-C4 bonds. On the other hand, the H···H interactions lead to the elongation of N-glycosidic bond.

REFERENCES

[1] M.R. Stratton, P.J. Campbell, P.A. Futreal, The Cancer Genome, Nature 458 (2009) 719.

[2] J.T. Stivers, A.C. Drohat, Arch. Biochem. Biophys. 396 (2001) 1.

[3] J.M. Lord, L.M. Roberts, J.D. Robertus, FASEB J. 8 (1994) 201.

[4] A. Bzowska, E. Kulikowska, D. Shugar, Pharmacol. Ther. 88 (2000) 349.

[5] R. Pellé, V.L. Schramm, D.W. Parkin, J. Biol. Chem. 273 (1998) 2118.

[6] W. Versées, S. Loverix, A. Vandemeulebroucke, P. Geerlings, J. Steyaert, J. Mol. Biol. 338 (2004) 1.

[7] T. Hollis, Y. Ichikawa, T. Ellenberger, EMBO J. 19 (2000) 758.

[8] A. Banerjee, W. Yang, M. Karplus, G.L. Verdine, Nature 434 (2005) 612.

[9] S.D. Bruner, D.P.G. Norman, G.L. Verdine, Nature 403 (2000) 859.

[10] A.B. Robertson, A. Klungland, T. Rognes, I. Leiros, Cell. Mol. Life Sic. 66 (2009) 981.

[11] R.N. Trivedi, X.H. Wang, E. Jelezcova, E.M. Goellner, J.B. Tang, R.W. Sobol, Mol. Pharmacol. 74 (2008) 505.

[12] M.S. Bobola, S. Varadarajan, N.W. Smith, R.D. Goff, D.D. Kolstoe, A. Blank, B. Gold, J.R. Silber, Clin.

Cancer Res. 13 (2007) 612.
[13] J. Paik, T. Duncan, T. Lindahl, B. Sedgwick, Clin. Cancer Res. 15 (2005) 10472.
[14] M. Arabski, R. Krupa, K. Wozniak, M. Zadrozny, J. Kasznicki, M. Zurawska, J. Drzewoski, Mutat. Res. 554 (2004) 297.
[15] J. Blasiak, M. Arabski, R. Krupa, K. Wozniak, J. Rykala, A. Kolacinska, Z. Morawiec, J. Drzewoski, M. Zadrozny, Mutat. Res. 554 (2004) 139.
[16] M.T. Bennett, M.T. Rodgers, A.S.H. Hebert, L.E. Ruslander, L. Eisele, A.C. Drohat, J. Am. Chem. Soc. 128 (2006) 12510.
[17] Y. Zheng, P. Cloutier, D.J. Hunting, L. Sanche, J.R. Wagner, J. Am. Chem. Soc. 127 (2005) 16592.
[18] Z. Li, Y. Zheng, P. Cloutier, L. Sanche, J.R. Wagner, J. Am. Chem. Soc. 130 (2008) 5612.
[19] M. Polak, K.L. Seley, J. Plavec, M. Polak, K.L. Seley, J. Plavec, J. Am. Chem. Soc. 126 (2004) 8159.
[20] M. Hennig, M.L. Munzarová, W. Bermel, L.G. Scott, V. Sklenář, J.R. Williamson, J. Am. Chem. Soc. 128 (2006) 5851.
[21] P. Hu, S. Wang, Y. Zhang, J. Am. Chem. Soc. 130 (2008) 16721.
[22] B.S. Plosky, E.G. Frank, D.A. Berry, G.P. Vennall, J.P. McDonald, R. Woodgate, Nucleic Acids Res. 34 (2006) 1070.
[23] P.J. O'Brien, T. Ellenberger, Biochem. 42 (2003) 12418.
[24] R. Rios-Font, L. Rodri-guez-Santiago, J. Bertran, M. Sodupe, J. Phys. Chem. B 111 (2007) 6071.
[25] M. Degano, S.D. Almo, J.C. Sacchettini, V.L. Schramm, Biochem. 37 (1998) 6277.
[26] V. Sychrovský, N. Müller, B. Schneider, V. Smrečki, V. Sÿpirko, J. Sponer, L. Trantírek, J. Am. Chem. Soc. 127 (2005) 14663.
[27] F. Sheng, X. Jia, A. Yep, J. Preiss, J.H. Geiger, J. Biol. Chem. 248 (2009) 17796.
[28] W.B.T. Cruse, P. Saludjian, Y. Leroux, G. Léger, D.E. Manouni, T. Prange, J. Biol. Chem. 271 (1996) 15558.
[29] W.K. Olson, J.L. Sussman, J. Am. Chem. Soc. 104 (1982) 210.
[30] E. Trottas, E. D'Ambrosio, N.D. Grossos, G. Ravagnans, M. Cirillin, M. Paci, J. Biol. Chem. 268 (1993) 3944.
[31] N. Foloppe, L. Nilsson, J. Phys. Chem. B 109 (2005) 9119.
[32] O.V. Shishkin, L. Gorb, O.A. Zhikol, J. Leszczynski, J. Biomol. Struct. Dynamics 22 (2004) 227.
[33] N. Foloppe, A.D. MacKerell, J. Phys. Chem. B 102 (1998) 6669.
[34] N. Foloppe, B. Hartmann, L. Nilsson, A.D. MacKerell, Biophys. J. 82 (2002) 1554.
[35] A.E. Reed, L.A. Curtiss, F. Weinhold, Chem. Rev. 88 (1988) 899.
[36] R.F.W. Bader, Atoms in Molecules: A Quantum Theory, Oxford University Press Oxford, 1990.
[37] N. Arul Murugan, H. Wilhelm Hugosson, J. Phys. Chem. B 113 (2009) 1012.
[38] J. Donohue, K.N. Trueblood, J. Mol. Biol. 2 (1960) 363.
[39] D. Touboul, G. Bouchoux, R. Zenobi, J. Phys. Chem. B 112 (2008) 11716.
[40] C. Altona, M. Sundaralingam, J. Am. Chem. Soc. 94 (1972) 8205.
[41] J.E. Kilpatrick, K.S. Pitzer, R. Spitzer, J. Am. Chem. Soc. 69 (1947) 2483.
[42] A.D. Becke, J. Chem. Phys. 98 (1993) 5648.
[43] M.J. Frisch et al., Gaussian 03 (Revision B.03) Gaussian, Inc, Pittsburgh, PA, 2003.
[44] E. Cancès, B. Mennucci, J. Tomasi, J. Chem. Phys. 107 (1997) 3032.
[45] E.D. Glendening, A.E. Reed, J.E. Carpenter, F. Weinhold, NBO Version 3.1, Theoretical Chemistry Institute, University of Wisconsin, Madison, 1990.
[46] F.W. Biegler König, J. Schönbohm, D. Bayles, J. Comput. Chem. 22 (2001) 545.
[47] P. Hobza, Phys. Chem. Chem. Phys. 3 (2001) 2555.